Nonlinear theory of particle drift in the field of resonant radiation

F. Kh. Gel'mukhanov and A. I. Parkhomenko

Institute of Automation and Electrometry, Siberian Branch of the Academy of Sciences of the USSR, Novosibirsk

(Submitted 27 June 1986)
Zh. Eksp. Teor. Fiz. **92**, 813–830 (March 1987)

A nonlinear theory of particle drift is proposed. Factors taken into account include light-induced drift, radiation pressure, and negative radiation pressure. The nonlinearity of the theory is due to the dependence of the drift velocity of the absorbing particles on the radiation intensity which, in turn, depends on the density of the absorbing gas. An analogy is found between particle drift in the radiation field and shock waves. In particular, it is shown that, in the case of an optically thin medium, light-induced drift and radiation pressure effects are described by the Burgers equation. Different types of particle-bunch drift are investigated, the conditions for the appearance of solitary waves are analyzed, and collisions between such waves are studied. It is shown that, in contrast to solitons, collision between the solitary waves investigated in this paper are entirely inelastic.

1. INTRODUCTION

The phenomenon of light-induced drift (LID) in gases[1] has recently attracted increasing attention among researchers, and a substantial number of theoretical and experimental papers have appeared in this field (see the bibliography in Ref. 2). The essence of the phenomenon is that resonant particles interacting with a traveling light wave, and colliding with buffer-gas particles, exhibit directed motion (drift) relative to the buffer gas. Calculations show that the drift velocity can reach values equal to the thermal velocity. The drift velocity attained experimentally[3] is 1.3×10^3 cm/s.

Theoretical papers devoted to LID have been largely concerned with studies of the effect under time-independent conditions. At the same time, from the point of view of experimental studies of LID and its possible practical applications (e.g., in isotope separation), there is considerable interest in the theoretical description of the dynamics of the variation in the macroscopic parameters of the absorbing gas during LID.

Consider a clump of the absorbing gas in a long cell filled with a buffer gas. Radiation propagates along the cell axis (z-axis) and brings the absorbing gas into motion. It then follows from the continuity equation ($\partial\rho/\partial t + \partial j/\partial z = 0$) and the expression for the current of the absorbing particles ($j = u\rho - D\partial\rho/\partial z$) that the density of the absorbing particles in space and its dependence on time are described by the equation

$$\frac{\partial\rho}{\partial t}+\frac{\partial(u\rho)}{\partial z}=\frac{\partial}{\partial z}\left(D\frac{\partial\rho}{\partial z}\right), \qquad (1.1)$$

where $\rho\equiv\rho(z,t)$ is the density, u is the LID velocity, and D is the diffusion coefficient of the absorbing particles in the buffer gas. When u = const, D = const, the solution of (1.1) subject to the initial condition $\rho(z,t=0) = \rho(z)$ is

$$\rho(\xi,t)=\int_{-\infty}^{\infty}\frac{\rho(\eta)\exp[-(\xi-\eta)^2/4Dt]}{(4\pi Dt)^{1/2}}d\eta, \quad \xi=z-ut, \qquad (1.2)$$

which describes the drift of the gas clump with velocity u, and its simultaneous spreading by diffusion. The light-induced drift of the particle clump was investigated experimentally in Ref. 3 for u and D varying slowly along the clump. The spreading of the clump by diffusion during the drift process was found to be satisfactorily described by (1.2).

In fact, the condition u = const is practically never satisfied exactly because the drift velocity varies across the clump as a result of absorption of radiation. The departure from the condition u = const should cause a departure from the spreading of the particle clump by diffusion in accordance with (1.2). In the experiments described in Ref. 3, the drift velocity varied slowly within the clump, and deviation from the diffusion-type spreading could be neglected. However, it is possible to experimentally establish conditions in which the drift velocity varies slowly and has a radical effect on the evolution of the particle clump, and so cannot be neglected. Actually, let us suppose that, for example, the variation of the drift velocity within the clump is such that its trailing edge (the edge on the side opposite to the direction of drift) drifts with a higher velocity than that of the leading edge, i.e., the bunch becomes compressed. After a certain interval of time, this drift compression and the usual diffusion spreading completely cancel out. In other words, the shape and width of the clump become stabilized and propagates in the form of a solitary wave. When the sign of the drift velocity is reversed, the bunch spreads more rapidly than in the case of ordinary diffusion.

It is important to note that, in general, the diffusion coefficient D of the absorbing particles is also a function of the radiation intensity. This affects, for example, the shape and width of the solitary wave but, in contrast to the case where $u\neq$ const, it cannot give rise to a qualitative change in the evolution of the drifting bunch. The change in D is usually small, so that quantitative changes in drift parameters are also small.

The present paper is devoted to a theoretical description of the drift dynamics of absorbing particles in which the change in the drift velocity due to the absorption of radiation is taken into account.

2. QUALITATIVE DESCRIPTION OF DRIFT DYNAMICS

Let us examine the dependence of drift velocity on radiation intensity. For completeness, we shall take into account

 0038-5646/87/030458-10$04.00

the effect of radiation pressure, although this is usually several orders of magnitude weaker than the LID effect.[4] In the case of homogeneous absorption-line broadening ($\Gamma \gg k\bar{v}$), it follows from the results reported in Ref. 5 that LID and light pressure effects cause the absorbing gas to drift with velocity

$$\mathbf{u}=\mathbf{u}_0\Phi_0(\varkappa)+\mathbf{u}_r\Phi_r(\varkappa), \tag{2.1}$$

where

$$\mathbf{u}_0=-\bar{v}\frac{\Delta\nu}{2\nu}\frac{\beta}{(1+\beta^{1/2})^2}\frac{\mathbf{k}\bar{v}\Omega}{\Gamma^2+\Omega^2}, \quad \mathbf{u}_r=\mathbf{v}_r\frac{\Gamma_1}{2\nu}, \quad \mathbf{v}_r=\frac{\hbar\mathbf{k}}{m},$$

$$\Phi_0(\varkappa)=\frac{\varkappa(1+\beta^{1/2})^2}{(1+\varkappa)(1+\beta\varkappa)},$$

$$\Phi_r(\varkappa)=\frac{\varkappa}{1+\varkappa}\left[1-\frac{\Delta\nu}{2\Gamma_1}\frac{\beta(2+\varkappa)}{1+\beta\varkappa}\right], \tag{2.2}$$

$$\beta=\frac{\Gamma_1}{\Gamma_1+\nu}, \quad \Delta\nu=\nu_1-\nu_0, \quad \varkappa=\frac{4|G|^2\Gamma}{\Gamma_1(\Gamma^2+\Omega^2)}, \quad G=\frac{d_{10}E}{2\hbar},$$

$$\Omega=\omega-\omega_{10}, \quad \nu\equiv\nu_1.$$

In these expressions, $\bar{v}$ is the most probable velocity of the absorbing particles, ω, k, E are, respectively, the frequency, wave vector, and electric field amplitude in the light wave, Γ is the homogeneous width of the absorption line, Γ_1 is the quenching constant in the excited state, ν_1 and ν_0 are the collision frequencies of excited and unexcited particles with buffer-gas particles, ω_{10} is the frequency of the transition between the ground (0) and excited (1) states, d_{10} is the matrix element of the dipole moment for the $1 \to 0$ transition, and m is the mass of the absorbing particle. For simplicity, Eqs. (2.2) are written for the case $|\Delta\nu|/\nu \ll 1$.

The drift velocity (2.1) consists of two terms. The first is proportional to Ω and describes the LID effect. The second is proportional to the recoil velocity v_r and is due to the radiation pressure. It describes both the radiation pressure effect proper[6] [first term in the function $\Phi_r(\varkappa)$] and the negative radiation pressure effect[5] [second term in $\Phi_r(\varkappa)$]. Figure 1 shows typical dependence of the drift velocity on $\varkappa$ in the case of LID [$\Phi_0(\varkappa)$] and in the case of light pressure [$\Phi_r(\varkappa)$].

The radiation pressure effect can be neglected when $\Omega \neq 0$. The situation is then dominated by the LID effect. Figure 1a shows the LID velocity as a function of radiation intensity, represented by the function $\Phi_0(\varkappa)$. For small $\varkappa$, we have $\Phi_0(\varkappa) \simeq \varkappa(1+\beta^{1/2})^2$, which depends linearly on the radiation intensity. As $\varkappa$ increases, the magnitude of the drift velocity becomes a maximum at $\varkappa_m = \beta^{-1/2}$ and behaves as $|u_0|(1+\beta^{1/2})^2/\beta\varkappa$ for $\varkappa \gg 1/\beta$. Depending on the sign of $\Omega\Delta\nu$, the drift of resonant particles can occur either in the direction of the light beam ($\Omega\Delta\nu < 0$), or in the opposite direction ($\Omega\Delta\nu > 0$). We note that this description of the behavior of the $\Phi_0(\varkappa)$ curve is typical for LID and remains qualitatively valid for any ratio of the homogeneous to the Doppler absorption linewidth.[7]

LID is absent in the case of precise resonance ($\Omega = 0$), and the particle drift is then due to the light pressure alone (Figs. 1b and c). The drift velocity becomes saturated for $\varkappa \gg 1$ (if $\Delta\nu = 0$) or for $\varkappa \gg 1/\beta$ (if $\Delta\nu \neq 0$). When $\Delta\nu/2\Gamma_1 < 1$, the drift velocity $\mathbf{u}$ always points along $\mathbf{k}$, and its dependence on the radiation intensity is described by curves 1, 2, or 3 (Fig. 1b), depending on the sign of $\Delta\nu$. When

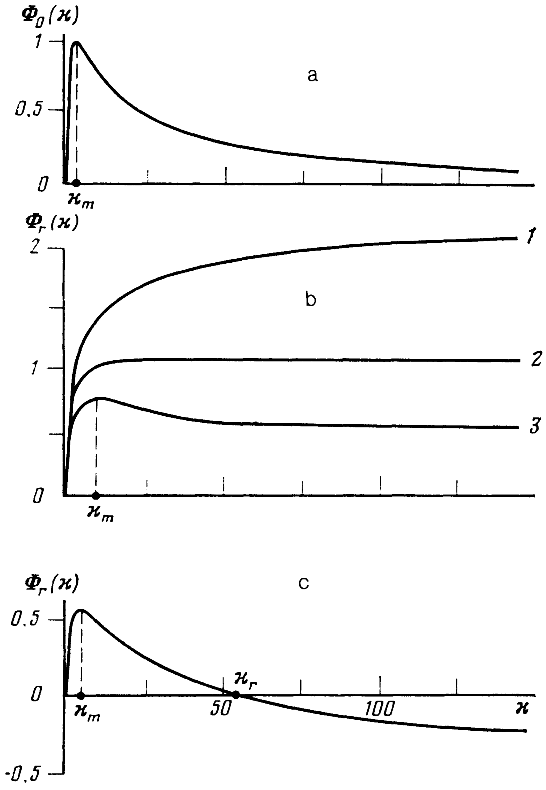

FIG. 1. Drift velocity as a function of radiation intensity: (a) LID effect, $\beta = 0.1$; (b) radiation pressure effect for $\Delta\nu/2\Gamma_1 < 1$. Curve 1—$\Delta\nu/\nu = -0.1$, $\Delta\nu/2\Gamma_1 = -1$, $\beta = 1/21$, 2—$\Delta\nu = 0$, 3—$\Delta\nu/\nu = 0.1$, $\Delta\nu/2\Gamma_1 = 0.5$, $\beta = 1/11$; (c) radiation pressure effect for $\Delta\nu/2\Gamma_1 > 1$, $\Delta\nu/\nu = 0.1$, $\Delta\nu/2\Gamma_1 = 1.5$, $\beta = 1/31$.

$\Delta\nu \leqslant 0$, the velocity $\mathbf{u}$ is found to increase with increasing $\varkappa$, whereas, for $\Delta\nu > 0$, the drift velocity reaches a maximum at $\varkappa = \varkappa_m$, and then decreases. The latter effect is due to the fact that negative radiation pressure becomes significant[5] for $\Delta\nu > 0$. When $\Delta\nu/2\Gamma_1 < 1$, this pressure partially cancels the usual radiation pressure. On the other hand, the situation is qualitatively different when $\Delta\nu/2\Gamma_1 > 1$ (see Fig. 1c), and the drift velocity $\mathbf{u}$ then points along $\mathbf{k}$ for small $\varkappa$. However, as the intensity increases, the usual light pressure is exactly cancelled by the negative light pressure at the point

$$\varkappa_r=\frac{1}{\beta(\Delta\nu/2\Gamma_1-1)} \tag{2.3}$$

i.e., the drift is shut off. A further increase in $\varkappa$ is accompanied by the drift of absorbing particles[5] in the direction antiparallel to $\mathbf{k}$.

Let us consider separately the special cases of small (optically thin medium) and large (optically dense medium) changes in drift velocity across the clump.

For the optically thin medium, the radiation intensity and, consequently, the drift velocity varies little from one end of the clump to the other. Let us suppose that $\Omega \neq 0$, i.e., LID is the predominant effect and the dependence of the drift velocity on $\varkappa$ is determined by the function $\Phi_0(\varkappa)$ (Fig. 1a). We shall see presently that the cases (1) $\mathbf{k}\cdot\mathbf{u} > 0$, $\varkappa_0 \leqslant \varkappa_m$ and (2) $\mathbf{k}\cdot\mathbf{u} < 0$, $\varkappa_0 > \varkappa_m$ correspond to the same evolution of the particle cloud ($\varkappa_0$ is the saturation parameter for radiation entering the clump), whereas (3) $\mathbf{k}\cdot\mathbf{u} < 0$, $\varkappa_0 \leqslant \varkappa_m$ and

(4) $\mathbf{k}\cdot\mathbf{u}>0$, $\varkappa_0>\varkappa_m$ are associated with a different type of evolution.

In case (1), the particles drift parallel to $\mathbf{k}$ and the drift velocity decreases across the clump, i.e., the trailing edge drifts faster than the leading edge (indicated by the arrows in Fig. 2a). When the difference between the drift velocities of the two fronts, $|\Delta u|$, is initially greater than the diffusion spreading velocity $u_{\rm dif}\sim D/a$ (a is the characteristic width of the clump), the trailing edge will catch up with the leading edge. The compression of the particle clump continues until the drift compression is balanced by diffusion spreading, i.e., until $|\Delta u|\sim D/a$. It follows that the shape and width of the particle clump will become stabilized after a finite time, and will then propagate in the form of a solitary wave, with the width remaining smaller than the original width of the clump. It will be shown below (see Section 4) that, in an optically thin medium, all the absorbing particles accumulate in the solitary wave. The characteristic size a_f of the resulting solitary wave is

$$a_f\sim D/|\Delta u|\sim\lambda\bar{v}/|\Delta u|, \tag{2.4}$$

where λ is the mean free path of the absorbing particles. Also, the time taken to form the solitary wave obviously satisfies:

$$t\gtrsim a_0/|\Delta u|, \quad a_f<a_0, \tag{2.5}$$

where a_0 is the initial characteristic width of the clump.

However, when the situation is such that, initially, $u_{\rm dif}>|\Delta u|$, the clump will initially spread out, reducing the velocity $u_{\rm dif}$ and, in the final analysis, the cancellation of the diffusion spreading by drift compression. This results in the formation of a solitary wave of width a_f (2.4) that is larger than the initial clump width a_0. The evolution time is

$$t\gtrsim a_f/u_{\rm dif}\approx a_f^2/D\sim D/(\Delta u)^2, \quad a_f>a_0. \tag{2.6}$$

When $u_{\rm dif}\sim|\Delta u|$ at the initial instant of time, the initial parameters of the clump will obviously change little during this process.

In case (2) ($\mathbf{k}\cdot\mathbf{u}<0$, $\varkappa_0>\varkappa_m$), the clump drifts in the direction opposite to that of $\mathbf{k}$, and the drift velocity of the leading edge is less than that of the trailing edge, just as in case (1) (indicated by the arrows in Fig. 2a). It follows that, here again, the shape and width of the drifting clump of particles are stabilized.

In the cases (3) ($\mathbf{k}\cdot\mathbf{u}<0$, $\varkappa_0>\varkappa_m$) and (4) ($\mathbf{k}\cdot\mathbf{u}>0$, $\varkappa_0>\varkappa_m$), the drift velocity of the leading edge is greater than that of the trailing edge (see Fig. 2b), which contrasts with cases (1) and (2). The gas bunch will therefore spread out more rapidly than in the case of ordinary diffusion (with velocity $u_{\rm dif}+|\Delta u|>u_{\rm dif}$).

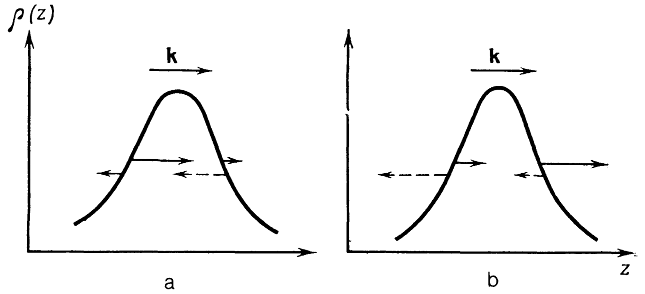

FIG. 2. Illustration of the stabilization (a) and spreading (b) of a drifting particle clump.

In this situation, when the particle drift is exclusively due to the radiation pressure effect ($\Omega=0$), the dependence of u on $\varkappa$ is determined by the function $\Phi_r(\varkappa)$ (Fig. 1b and c). Proceeding in a similar way, we arrive at the following. When $\Delta\nu\leqslant0$ and $\Delta\nu>0$, $\varkappa_0\leqslant\varkappa_m$, the shape and width of the particle clump become stabilized. On the other hand, when $\Delta\nu>0$, $\varkappa_0>\varkappa_m$, the spreading of the clump is faster than that in ordinary diffusion (it occurs with velocity $u_{\rm dif}+|\Delta u|>u_{\rm dif}$.

New features arise as we pass from an optically thin to an optically thick medium. Let us suppose, for example, that the dependence of u on $\varkappa$ is described by the function $\Phi_r(\varkappa)$ with $\Delta\nu/2\Gamma_1>1$ (Fig. 1c) and that $\varkappa_0>\varkappa_r$, $\varkappa_f<\varkappa_m$, where $\varkappa_f$ is the saturation parameter as the radiation leaves the gas clump. The particle drift velocity within the clump will vary as follows. The drift velocity of the trailing edge (where $\varkappa\sim\varkappa_0$) points in the opposite direction to that of $\mathbf{k}$. As the radiation intensity decreases inside the clump, the drift velocity eventually vanishes and then, having changed its direction, begins to increase, reaching a maximum in the part of the clump in which $\varkappa=\varkappa_m$. The drift velocity then falls in the direction of the leading edge (where $\varkappa\sim\varkappa_f$). The trailing edge (where $\varkappa>\varkappa_m$) is thus seen to spread out more rapidly than in ordinary diffusion. Moreover, the region in this part of the clump in which $\varkappa>\varkappa_r$ will drift antiparallel to $\mathbf{k}$, whereas the region with $\varkappa<\varkappa_r$ will drift in the direction of $\mathbf{k}$. The front of the clump (in which $\varkappa<\varkappa_m$) will propagate in the form of a solitary wave after a certain interval of time. However, this wave will not collect all the particles of the initial clump (when $\varkappa_0\leqslant\varkappa_m$, the solitary wave will, of course, capture all the particles).

When we analyze the dependence of u on $\varkappa$, we readily see that, in an optically thick medium, in which $\varkappa_0>\varkappa_m>\varkappa_f$, the original clump partly changes into a solitary wave both in the case of the radiation pressure effect with $\Delta\nu>0$ and in the case of the LID. The only exception is the case of drift under radiation pressure for $\Delta\nu\leqslant0$. In the latter case, the solitary wave always collects all the particles of the original bunch.

3. BURGERS EQUATION

Let us now consider the one-dimensional problem. This is valid when the radiation intensity is distributed uniformly across the gas-filled cell. The radiation propagates along the cell axis (z-axis). The drift of the absorbing gas is described by the continuity equation

$$\partial\rho/\partial t+\partial j/\partial z=0, \tag{3.1}$$

where the current of absorbing particles (see Appendix) is given by

$$j=u\rho-D(\partial\rho/\partial z), \quad D=\bar{v}^2/2\nu \tag{3.2}$$

and the drift velocity u is given by (2.1) and (2.2). Since the drift velocity (2.1) depends on the radiation intensity, Eqs. (3.1) and (3.2) must be supplemented by the equation for the radiation intensity, or the saturation parameter[4] $\varkappa$,

$$\partial\varkappa/\partial z=-\sigma\varkappa\rho/(1+\varkappa), \tag{3.3}$$

where σ is the photoabsorption cross section.

The solution of (3.3) is

$$\ln\frac{\varkappa(z,t)}{\varkappa_0}+\varkappa(z,t)-\varkappa_0=-\sigma N(z,t),$$
$$N(z,t)=\int_{-\infty}^{z}\rho(\xi,t)\,d\xi,\quad \varkappa_0\equiv\varkappa(-\infty). \tag{3.4}$$

The value $\varkappa_0$ of the saturation parameter for $z=-\infty$ is independent of time since we are interested in finite times for which the gas bunch has not reached the point $z=\pm\infty$. For the same reason, the particle current will be zero at $z=-\infty$, i.e., $j(-\infty,t)=0$. This also means that the other physical parameters are time-independent at $z=\pm\infty$. We shall therefore omit the argument t for $z=\pm\infty$, e.g., we shall write

$$u(\pm\infty,t)=u(\pm\infty),\quad N(\infty,t)=N(\infty).$$

Since the saturation parameter $\varkappa(z,t)$ depends on $N(z,t)$, it will be useful to transform from the density $\rho(z,t)$ to $N(z,t)$ in (3.1). Bearing (3.2) in mind, we therefore integrate (3.1) with respect to z:

$$\frac{\partial N(z,t)}{\partial t}+u(z,t)\frac{\partial N(z,t)}{\partial z}=D\frac{\partial^2N(z,t)}{\partial z^2}. \tag{3.5}$$

This is a nonlinear equation because $u(z,t)$ is shown by (2.1) and (3.4) to be a function of $N(z,t)$. We have not been able to solve this equation in the general case. There is, however, a physically important limiting case for which an exact solution of (3.5) is available. This is the limit of an optically thin medium:

$$\sigma N\ll 1,\quad N=N(\infty). \tag{3.6}$$

When this condition is satisfied, the radiation intensity and, consequently, the drift velocity depend weakly on $N(z,t)$. We can therefore expand $u(z,t)$ in powers of $\sigma N(z,t)$. To first order in the small parameter (3.6), we have

$$u(z,t)=u(-\infty)-\Delta uN(z,t)/N, \tag{3.7}$$

where we have introduced the velocity jump

$$\Delta u=u(-\infty)-u(\infty)=u(-\infty)\bar{\sigma}N \tag{3.8}$$

across the gas clump. Expressions for $u(-\infty)$ and σ are obtained directly from (2.1), (2.2), and (3.4):

$$u(-\infty)=u_0(-\infty)+u_r(-\infty),\quad \bar{\sigma}=\frac{u_0(-\infty)\bar{\sigma}_0+u_r(-\infty)\bar{\sigma}_r}{u(-\infty)},$$
$$u_0(-\infty)=u_0\Phi_0(\varkappa_0),\quad u_r(-\infty)=u_r\Phi_r(\varkappa_0),$$
$$\bar{\sigma}_0/\sigma=(1-\beta\varkappa_0^2)/(1+\varkappa_0)^2(1+\beta\varkappa_0), \tag{3.9}$$
$$\frac{\bar{\sigma}_r}{\sigma}=\left\{1-\frac{\Delta\nu\beta}{2\Gamma_1(1+\beta\varkappa_0)^2}[2(1+\varkappa_0)+\varkappa_0^2(1-\beta)]\right\}$$
$$\times\left\{(1+\varkappa_0)^2\left[1-\frac{\Delta\nu\beta}{2\Gamma_1}\frac{2+\varkappa_0}{1+\beta\varkappa_0}\right]\right\}^{-1}.$$

Multiplying (3.5) by $\partial u(z,t)/\partial N(z,t)$ and recalling that $\partial^2u(z,t)/\partial N^2(z,t)=0$ by virtue of (3.7), we find that

$$\frac{\partial u(z,t)}{\partial t}+u(z,t)\frac{\partial u(z,t)}{\partial z}=D\frac{\partial^2u(z,t)}{\partial z^2}. \tag{3.10}$$

This is the well-known Burgers equation[8,9] of shock-wave physics. It is clear from (3.7) that an equation identical to (3.10) is valid for $N(z,t)$. It is readily seen that the total number of particles

$$N=N(\infty,t)<\infty \tag{3.11}$$

is an integral of (3.10).

Using the Cole-Hopf transformation[8,9]

$$u(z,t)=-2D\frac{\partial}{\partial z}\ln\psi(z,t) \tag{3.12}$$

we can reduce the Burgers equation (3.10) to the diffusion equation

$$\frac{\partial\psi(z,t)}{\partial t}=D\frac{\partial^2\psi(z,t)}{\partial z^2}. \tag{3.13}$$

The solution of this equation, subject to the initial condition

$$u(z,0)=u(-\infty)-\frac{\Delta u}{N}\int_{-\infty}^{z}\rho(x,0)\,dx \tag{3.14}$$

is

$$\psi(z,t)=\exp\left(-\frac{u_c^2t}{4D}-\frac{z_cu_c}{2D}\right)\int_{-\infty}^{\infty}d\eta$$
$$\times\exp\left[-\frac{(z_c-\eta)^2}{4Dt}-\frac{\Delta u}{2D}\left\{\frac{\eta}{2}-\frac{1}{N}\int_0^{\eta}dx\int_{-\infty}^{x}d\xi\,\rho(\xi,0)\right\}\right](4\pi Dt)^{-1/2}, \tag{3.15}$$

where we have introduced the drift velocity of the center of gravity of the absorbing particles, u_c, and the coordinate z_c in the center-of-gravity system:

$$u_c=\frac{1}{N}\int_{-\infty}^{\infty}u(z,t)\rho(z,t)\,dz=\frac{u(-\infty)+u(\infty)}{2}$$
$$=u(-\infty)-\frac{\Delta u}{2}, \tag{3.16}$$
$$z_c=z-\bar{z}-u_ct,\quad \bar{z}=\frac{1}{N}\int_{-\infty}^{\infty}z\rho(z,0)\,dz.$$

The solution given by (3.15) enables us to find the drift velocity (3.12) and the density distribution of the absorbing gas:

$$\rho(z,t)=-\frac{N}{\Delta u}\frac{\partial u(z,t)}{\partial z}. \tag{3.17}$$

It is important to note that (3.8) and (3.17) were used to obtain the expression for u_c given by (3.16).

4. EVOLUTION OF A SINGLE PARTICLE CLUMP

Before we investigate the propagation of an individual clump of absorbing particles, let us examine the behavior of the solution of (3.10) for large t. The solution given by (3.15) contains three time scales, namely,

$$t_0=a^2/D,\quad t_1=a/|\Delta u|,\quad t_2=D/(\Delta u)^2, \tag{4.1}$$

where a is the characteristic scale of the density gradient. If we have a sufficiently narrow initial distribution of absorbing particles with effective size a_0, such that

$$a_0 \ll D/|\Delta u|, \tag{4.2}$$

then,

$$t_0 \ll t_1 \ll t_2. \tag{4.3}$$

When (4.2) is valid and

$$t \gg t_0 \tag{4.4}$$

the solution given by (3.15) assumes the following asymptotic form:

$$\psi(z,t)=\exp\left(-\frac{u_c^2 t}{4D}-\frac{z_c u_c}{2D}\right) \times \int_{-\infty}^{\infty} d\eta \exp\left[-\frac{(z_c-\eta)^2}{4Dt}+\frac{\Delta u|\eta|}{4D}\right](4\pi Dt)^{-1/2}. \tag{4.5}$$

Let us express this integral in terms of the error integral

$$\operatorname{erf}(x)=\frac{2}{\pi^{1/2}}\int_0^x e^{-\xi^2} d\xi$$

and transform in (3.12) and (3.17) to the dimensionless variables x and τ:

$$x=z_c/l=(z-\bar{z}-u_c t)/l, \quad \tau=t u_c^2/D, \quad l=D/u_c. \tag{4.6}$$

In the frame in which the center of gravity of the bunch is at rest, we then have the following expressions for the drift velocity $u'(x,\tau)$ and density $\rho(x,\tau)$ of the absorbing particles:

$$u'(x,\tau)/u_c=[u(x,\tau)-u_c]/u_c=\alpha(1-Q)/(1+Q),$$

$$\rho(x,\tau)=\frac{N}{l}\frac{Q}{(1+Q)^2}\left[\alpha+(1+Q) \times \exp\left\{-\left(\frac{x+\tau\alpha}{2\tau^{1/2}}\right)^2\right\}(\pi\tau)^{-1/2} \times \left\{1+\operatorname{erf}\left(\frac{x+\tau\alpha}{2\tau^{1/2}}\right)\right\}^{-1}\right], \tag{4.7}$$

where

$$Q=qe^{\alpha x}, \quad q=\left[1+\operatorname{erf}\left(\frac{x+\tau\alpha}{2\tau^{1/2}}\right)\right]\left[1-\operatorname{erf}\left(\frac{x-\tau\alpha}{2\tau^{1/2}}\right)\right]^{-1},$$

$$\alpha=\frac{\Delta u}{2u_c}. \tag{4.8}$$

It is clear from (4.1) and (4.4) that (4.5) and (4.7) become exact as $a_0 \to 0$, i.e., for a δ-function initial condition [see, however, the explanation of (A3)]:

$$\rho(z,0)=N\delta(z-\bar{z}), \quad N=\rho_0 a_0 \pi^{1/2}. \tag{4.9}$$

Let us examine our solution in greater detail. It is important to note the symmetry property of the asymptotic expression (4.7)

$$u'(x,\tau)=-u'(-x,\tau), \quad \rho(x,\tau)=\rho(-x,\tau), \tag{4.10}$$

which is exact for all τ, provided the initial distribution is symmetric, i.e., provided $\rho(z,0)=\rho(-z,0)$. The value of u' and ρ at the center of gravity of the bunch is an important parameter of (4.7):

$$u'(0,\tau)=0, \quad \rho(0,\tau)=\frac{N}{4l}\left[\alpha+\frac{2\exp(-\tau\alpha^2/4)}{(\pi\tau)^{1/2}(1+\operatorname{erf}(\tau^{1/2}\alpha/2))}\right]. \tag{4.11}$$

When $\tau\alpha^2/4 \ll 1$, the clump amplitude

$$\rho(0,\tau)=N/2l(\pi\tau)^{1/2} \tag{4.12}$$

increases without limit as $\tau \to 0$. This behavior of the density distribution is explained by the fact that, as is clear from (4.1) and (4.4), the limit as $\tau \to 0$ corresponds to a δ-function initial distribution (4.9). As time increases, the clump density $\rho(0,\tau)$ begins to depend strongly on the sign of α. In fact, it follows from (4.11) that

$$\rho(0,\tau)=\frac{N}{4l}\begin{cases}\dfrac{2}{\tau|\alpha|}, & \alpha<0, \quad \tau\alpha^2/4 \gg 1,\\ \dfrac{2}{(\pi\tau)^{1/2}}, & \alpha=0,\\ \alpha+\dfrac{\exp(-\tau\alpha^2/4)}{(\pi\tau)^{1/2}} \approx \alpha, & \alpha>0, \quad \tau\alpha^2/4 \gg 1.\end{cases} \tag{4.13}$$

The case $\alpha=0$ corresponds to ordinary diffusive $(1/\tau^{1/2})$ spreading of the drifting particle clump. If the drift velocity increases over the thickness of the gas clump, the velocity jump Δu is negative, i.e., $\alpha<0$. The trailing edge of the clump then lags behind the leading edge, and the initial distribution spreads out more rapidly than in the case of ordinary diffusion, and follows the drift law $1/\tau$. The reduction in the drift velocity from one side of the clump to the other $(\alpha>0)$ signifies that the trailing edge of the clump must catch up with the leading edge. However, diffusion will ensure that the clump shape will be stabilized, and its maximum density will tend to a constant value (see Fig. 3). A detailed qualitative picture of the drift spreading and compression of a particle clump is given in Section 2.

It follows directly from (4.7) that the solitary wave

$$\rho(x,\tau)=\frac{\alpha N}{2l}\frac{1}{1+\cosh(\alpha x)}, \quad \frac{\tau\alpha^2}{4} \gg 1 \tag{4.14}$$

will evolve out of any initial distribution for $\alpha>0$. This distribution was first obtained by Kuščer and Nienhuis[10] for

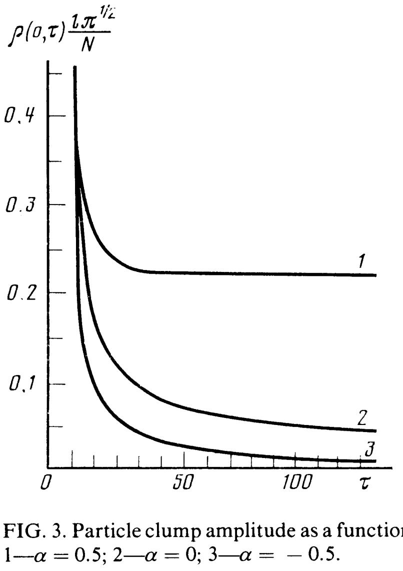

FIG. 3. Particle clump amplitude as a function of time: $\tau=u_c^2 t/D$. Curve 1—$\alpha=0.5$; 2—$\alpha=0$; 3—$\alpha=-0.5$.

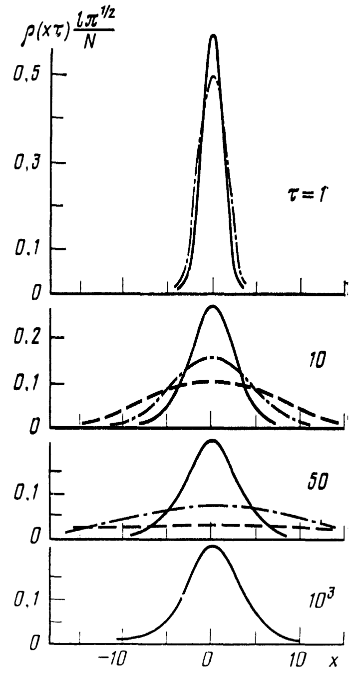

FIG. 4. Evolution of a single particle clump. The width a_0 of the initial distribution is less than the width $D/\Delta u$ of the solitary wave: solid curve—$\alpha = 0.5$; dot-dash curve—$\alpha = 0$; dashed curve—$\alpha = -0.5$.

the LID effect under weak-field conditions.

Figure 4 shows the time-dependence of the density of the absorbing particles, calculated from (4.7). This figure and (4.7) correspond to the limit of a narrow initial distribution (4.2). Comparison of (4.14) with (4.2) will readily show that we have examined the situation in which the width of the initial distribution a_0 was smaller than the width $D/|\Delta u|$ of the solitary wave (4.14).

Figure 5 shows the evolution of the solitary wave when its width $D/|\Delta u|$ is smaller than the width a_0 of the initial distribution. The calculations were based on (3.12) and (3.17) with the Gaussian initial distribution

$$\rho(z,\ 0)=\rho_0 \exp\left(-z^2/a_0^2\right), \tag{4.15}$$

for which the function $\psi(z,t)$ in (3.15) is given by

$$\psi(z,t)=\frac{1}{(4\pi Dt)^{1/2}}\exp\left(-\frac{u_c^2 t}{4D}-\frac{z_c u_c}{2D}\right)\int\limits_{-\infty}^{\infty} d\eta$$

$$\times\exp\left[-\frac{(z_c-\eta)^2}{4Dt}+\frac{\Delta u a_0}{4D}\left\{\frac{\eta}{a_0}\operatorname{erf}\left(\frac{\eta}{a_0}\right)\right.\right.$$

$$\left.\left.+\frac{\exp(-\eta^2/a_0^2)-1}{\pi^{1/2}}\right\}\right]. \tag{4.16}$$

It is clear from Fig. 5 that, when $\alpha > 0$, the Gaussian distribution (4.15) shrinks and deforms into the solitary wave (4.14). The question is whether it is possible to choose an initial distribution $\rho(z,0)$ that will remain unchanged during the particle drift process. The answer to this question is that this *is* possible. When $\alpha > 0$, (4.14) is a distribution of this kind (see also Section 6). The Gaussian distribution (4.15) with $a_0 = 8D/\pi^{1/2}\Delta u$ will also exhibit a very small change.

To conclude this Section, we note the following important point. It follows directly from (4.14) that the area under the solitary wave is equal to N (3.11). In other words, for an optically thin medium (3.6) with $u(z,t)/N(z,t) \neq 0$, the solitary wave captures all the absorbing particles. It is clear that this result does not follow from particle number conservation (N = const). It was shown in Section 2 that the only possible situation is that involving the partial capture of particles by the solitary wave. The remaining particles that are not confined by the radiation are then found to spread out along the entire length of the cell.

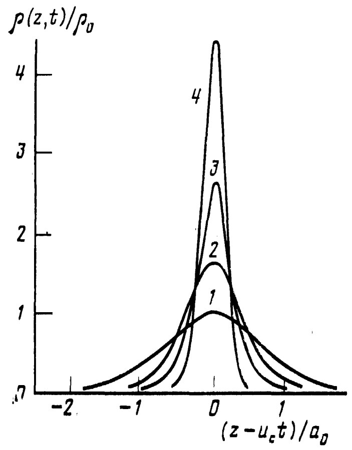

FIG. 5. Evolution of a single particle clump. The width a_0 of the initial distribution is greater than $D/\Delta u$ of the solitary wave. $\alpha = 0.1$; $u_c a/2D = 50$; $t' = t\Delta u/a_0$. Curve 1—$t' = 0$; 2—$t' = 1$; 3—$t' = 2$; 4—$t' > 10$.

5. SIMULTANEOUS PROPAGATION OF TWO PARTICLE CLUMPS

Let us consider the evolution of two clumps of absorbing particles

$$\rho(z,\ 0)=\rho_1(z,\ 0)+\rho_2(z,\ 0), \tag{5.1}$$

whose centers of gravity at $t = 0$ lie at $\bar z_1$ and $\bar z_2$. We shall assume that the distance $L = \bar z_2 - \bar z_1$ between the centers of gravity of the clumps for $t = 0$ is much greater than the characteristic width a_0 of the individual clumps. The initial distributions $\rho_1(z,0)$ and $\rho_2(z,0)$ will be assumed to be sufficiently narrow to ensure that (4.2) is satisfied. It can be shown that, when $t \gg a_0^2/D$, the solution (3.15) of the Burgers equation subject to the initial condition (5.1) has the following asymptotic form:

$$2\psi(z,t)=\left[1-\operatorname{erf}\left(\frac{z-\bar z_1-tu_-}{(4Dt)^{1/2}}\right)\right]\exp\left\{-\frac{u_-}{2D}\left(z-\frac{tu_-}{2}\right)\right\}$$

$$+\left[\operatorname{erf}\left(\frac{z-\bar z_1-tu}{(4Dt)^{1/2}}\right)-\operatorname{erf}\left(\frac{z-\bar z_2-tu}{(4Dt)^{1/2}}\right)\right]$$

$$\times\exp\left\{-\frac{\bar z_1\Delta u_1+(z-tu/2)u}{2D}\right\}$$

$$+\left[1+\operatorname{erf}\left(\frac{z-\bar z_2-tu_+}{(4Dt)^{1/2}}\right)\right]$$

$$\times\exp\left\{-\frac{\bar z_1\Delta u_1+\bar z_2\Delta u_2+(z-tu_+/2)u_+}{2D}\right\}, \tag{5.2}$$

where

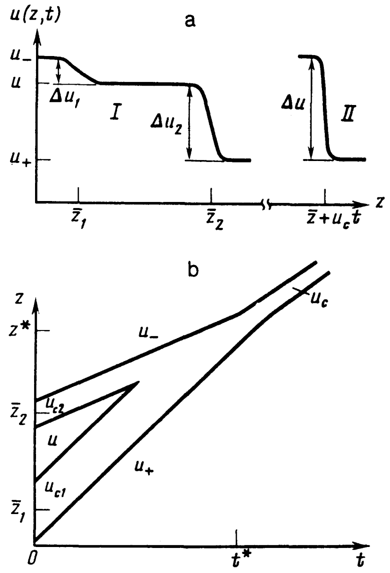

FIG. 6. (a) Drift velocity $u(z,t)$ as a function of z for (3.6); $L \gg a_0$, $\tilde\sigma > 0$. (I) $t = 0$; (II) $t \gg L/\Delta u$. (b) Analogy with the collision between two shock waves.

$$\bar z_i = \frac{1}{N_i}\int\limits_{-\infty}^{\infty} z\rho_i(z,0)\,dz,\quad N_i = \int\limits_{-\infty}^{\infty}\rho_i(z,0)\,dz,$$
$$\bar z_2 - \bar z_1 = L,\qquad i = 1, 2. \tag{5.3}$$

The physical significance of the drift velocities

$$u_\pm = u(\pm\infty),\quad u = u(\bar z_1 + L/2,\ 0) = u_- + \Delta u_1 \tag{5.4}$$

in (5.2) can readily be understood by examining Fig. 6a. The drift-velocity jumps Δu_1, Δu_2, and Δu, introduced in (5.4), and shown in Fig. 6a, are defined by

$$\Delta u_1 = u_- - u = u_-\tilde\sigma N_1,\quad \Delta u_2 = u - u_+ = u\tilde\sigma N_2,$$
$$\Delta u = \Delta u_1 + \Delta u_2 = u_-\tilde\sigma N,\quad N = N_1 + N_2. \tag{5.5}$$

They are the velocity jumps across the first, second, and the two clumps together, respectively.

Let us begin with the case

$$L\Delta u/D \gg 1,\quad \Delta u_i > 0. \tag{5.6}$$

This corresponds to the situation where the widths of the two solitary waves, $D/\Delta u_i$, are small in comparison with L. In other words, for times in the range

$$L/\Delta u \gg t \gg D/(\Delta u)^2 \tag{5.7}$$

we can speak of the evolution of individual clumps of the form (4.14) that have not as yet collided with one another. It is clear that, so long as (5.7) and $t \gg a_0^2/D$ are satisfied, the density distribution $\rho(z,t)$ takes the form of the sum of the two nonoverlapping distributions [$\rho_1(z,t)\,\rho_2(z,t) = 0$]

$$\rho(z,\ t) = \rho_1(z,\ t) + \rho_2(z,\ t), \tag{5.8}$$

whose shape is described by (4.14). However, the centers of gravity of each of the clumps, $\bar z_i$ ($i = 1.2$), and the parameters

$$u_{ci} = \frac{1}{N_i}\int\limits_{-\infty}^{\infty} u(z,t)\rho_i(z,t)\,dz,\quad \alpha_i = \frac{\Delta u_i}{2u_{ci}},\quad l_i = \frac{D}{u_{ci}} \tag{5.9}$$

that appear in (4.14) are then different for the two distributions $\rho_1(z,t)$ and $\rho_2(z,t)$. By analogy with (3.16), we can readily show that

$$u_{c1} = (u_- + u)/2 = u_- - \Delta u_1/2,\quad u_{c2} = (u + u_+)/2 = u_+ + \Delta u_2/2. \tag{5.10}$$

It is clear that a new solitary density wave (4.14) will arise after the two clumps collide [this follows from the exact solution (5.2)] for which the parameters of the center of gravity are

$$u_c = (N_1u_{c1} + N_2u_{c2})/N = (u_- + u_+)/2 = u_- - \Delta u/2,$$
$$\bar z = (N_1\bar z_1 + N_2\bar z_2)/N,\quad \alpha = \Delta u/2u_c,\quad l = D/u_c. \tag{5.11}$$

The single-wave situation described by (4.14) and (5.10) occurs for times $t \gg L/\Delta u$.

It is appropriate to note here the analogy with the collision of two shock waves. It is clear from (5.10) that, prior to collision between the clumps, their velocities u_{ci} are equal to the half-sum of the drift velocities before and after the clump $\rho_i(z,t)$. The result of the collision is that the particle clumps coalesce and the resulting single clump propagates with velocity u_c equal to the half-sum of the drift velocities before the first clump, u_-, and after the second clump, u_+ (see Fig. 6b). The amplitude of the resulting clump $\rho(0,t) = \Delta uN/8D$ is then greater than the amplitude of the initial clumps $\rho_i(0,t) = \Delta u_iN_i/8D$, and its width $D/\Delta u$ is smaller than the width $D/\Delta u_i$ of the initial clumps. It follows from Fig. 6b that the two solitary waves coalesce into one at time t^* at the point z^*. These quantities are given by the following approximate formulas:

$$t^* = 2L/\Delta u,\quad z^* - \bar z_1 = L(u_- + u)/\Delta u. \tag{5.12}$$

As indicated in the derivation of (5.2), this formula is asymptotic ($t \gg a_0^2/D$). It is important to note that (5.2) is the exact solution of the diffusion equation (3.13) for δ-function initial distribution

$$\rho(z,\ 0) = N_1\delta(z - \bar z_1) + N_2\delta(z - \bar z_2). \tag{5.13}$$

The expressions for $u(z,t)$ and $\rho(z,t)$, deduced on the basis of (5.2), are relatively complicated and we shall therefore confine our attention to the special case

$$N_1 = N_2 = N/2. \tag{5.14}$$

Using this condition, we find that the formula for the drift velocity can be obtained from (5.2), (3.12), and (3.17) in the form

$$\frac{u(x,\tau) - u_+}{2u_c} = \frac{\alpha}{\Delta}\left[1 - R + \frac{E(F-B)}{2}\right] \tag{5.15}$$

and the density of the absorbing particles is

$$\rho(x,\tau) = \frac{\alpha N}{l\Delta^2}\left[\frac{E}{4}(F-B)(1-R+\mathscr{D}) + \mathscr{D}(1-R)\right]$$
$$+ \frac{N}{l\Delta(\pi\tau)^{1/2}}\left[\exp(r^2) + \frac{E}{2}\{\exp(-b^2) - \exp(f^2)\}\right], \tag{5.16}$$

where

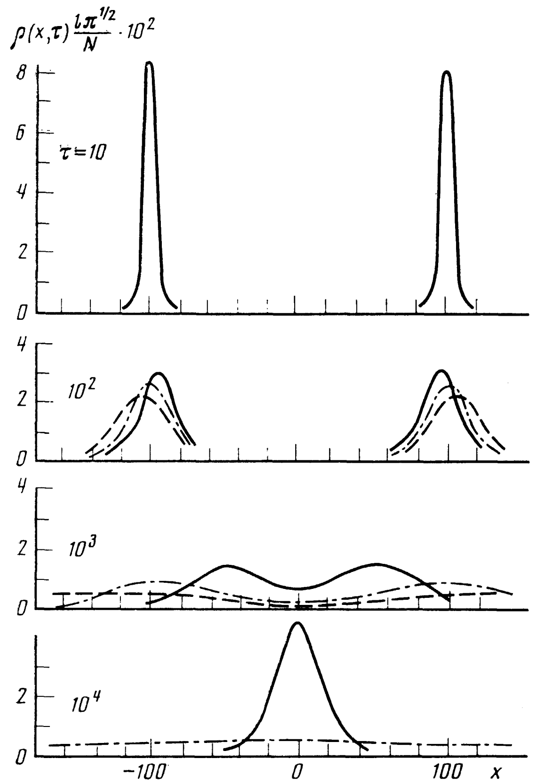

FIG. 7. Evolution of two particle clumps: $L\Delta u/D \gg 1$, $\tau = u_c^2 t/D$, $L/l = 200$, $l = D/u_c$, $\alpha = \Delta u/2u_c$. Solid curve—$\alpha = 0.1$, dot-dash curve $\alpha = 0$, dashed curve—$\alpha = -0.1$.

$$\Delta = 1 - R + \mathscr{D} + E(F-B), \quad R = \operatorname{erf}(r), \quad F = \operatorname{erf}(f), \quad B = \operatorname{erf}(b),$$

$$\mathscr{D} = \left[1 + \operatorname{erf}\left(b + \frac{\tau^{1/2}\alpha}{2}\right)\right]\exp(\alpha x),$$

$$E = \exp\left[\frac{\alpha}{2}\left(x + S - \frac{\tau\alpha}{2}\right)\right], \tag{5.17}$$

$$f = (x+S)/2\tau^{1/2}, \quad b = (x-S)/2\tau^{1/2}, \quad r = f - \tau^{1/2}\alpha/2,$$
$$S = L/2l, \quad x = (z - \bar{z} - tu_c)/l.$$

The remaining quantities in (5.15) and (5.16) are given by (5.11).

Figure 7 shows the results of calculations based on (5.16). The special case $\alpha = 0$ corresponds to the usual diffusive spreading of the two clumps that are at rest relative to each other in the frame in which the center of gravity is at rest. When $\alpha = 0$, the second clump lags behind the first. In this situation, the two clumps "repel" and spread out by diffusion. When $\alpha > 0$, the velocity of the second clump is greater than that of the first, and the former catches up with the latter. The clumps collide and coalesce. The collision results in a single clump (4.14), which is narrower and has a higher density. Its area is equal to the sum of the areas of the initial clumps. Figure 7 demonstrates the qualitative difference between the collision of clumps (for $\alpha > 0$) and the collision of ordinary solitons.[8,9] In contrast to solitons, which collide perfectly elastically,[8,9] the collision between the solitary waves considered here is perfectly inelastic.

6. THE CASE $\partial u(z,t)/\partial N(z,t) = 0$

So far, we have confined our attention to the situation where $\partial u(z,t)/\partial N(z,t) \neq 0$. The case in which

$$\partial u(z,t)/\partial N(z,t) = 0 \tag{6.1}$$

is more complicated, but it, too, is amenable to quantitative analysis, at least partially. To investigate the state defined by (6.1), it is convenient to rewrite (3.5) in the frame of reference moving with constant velocity u:

$$\frac{\partial N(\xi,t)}{\partial t} + (u(\xi,t) - u)\frac{\partial N(\xi,t)}{\partial \xi} = D\frac{\partial^2 N(\xi,t)}{\partial \xi^2},$$
$$\xi = z - ut. \tag{6.2}$$

Expanding $u(\xi,t)$ in a series in powers of the small parameter σN (3.6), retaining only the first nontrivial term in this expansion, and using (6.1), we obtain

$$u(\xi,t) = u(-\infty) - 3\Delta u \frac{N^2(\xi,t)}{N^2}, \tag{6.3}$$

where the expression for Δu is reproduced below for the LID effect alone:

$$\Delta u = \beta^{3/2}\sigma^2 u(-\infty)/3(1+\beta^{1/2})^4, \quad u(-\infty) = u_0\Phi_0(\varkappa_0). \tag{6.4}$$

Equations (6.2) and (6.3) cannot be solved in the general case. However, the situation is significantly simplified if we seek a solution in the form of a traveling wave $N(\xi,t) = N(\xi)$. From (6.2) and (6.3), we then have

$$N(\xi) = N\exp\{\mu(\xi-\xi_0)/2\}/[2+\exp\{\mu(\xi-\xi_0)\}]^{1/2}. \tag{6.5}$$

Hence, using (6.3), we can readily show that

$$u(\xi) - u = 2\Delta u\frac{1-\exp\{\mu(\xi-\xi_0)\}}{2+\exp\{\mu(\xi-\xi_0)\}}$$
$$\rho(\xi) = N\mu\frac{\exp\{\mu(\xi-\xi_0)/2\}}{[2+\exp\{\mu(\xi-\xi_0)\}]^{3/2}}. \tag{6.6}$$

where

$$u = u(-\infty) - \frac{\Delta u}{3}, \quad \mu = \frac{2\Delta u}{D},$$
$$\xi_0 = \frac{1}{\mu}\ln\left\{\frac{(N/N(0))^2 - 1}{2}\right\}. \tag{6.7}$$

The formulas given by (6.6) become meaningless when $\mu < 0$, as can be seen from the expression for $\rho(\xi)$. This is so because the state with $\mu < 0$ corresponds to the situation [see (6.3)], in which the trailing edge of the particle clump moves more slowly than the leading edge. The initial clump then spreads out [$\rho(\xi,t) \to 0$ for $t \to \infty$] and a stable structure, such as (6.6), is not produced. If, on the other hand, $\mu > 0$, the trailing edge of the clump catches up with the leading edge and the solitary wave (6.6) is produced.

It is important to note that the form of the clump $\rho(\xi)$, given by (6.6), is not the same as (4.14). In contrast to (4.14), the distribution (6.6) is asymmetric (see Fig. 8) and, as can be seen from (6.5), the area of the clump, $N(\infty)$, is equal to N. It follows that all the absorbing particles are trapped in the solitary wave (6.6), as they are in the solitary wave (4.14).

Clearly, the initial distribution $\rho(z,0) = \rho(z)$ with

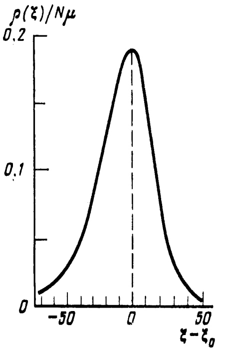

FIG. 8. Shape of solitary wave for $\partial u(z,t)/\partial N(z,t) = 0$; $\alpha = 0.1$.

$\mu > 0$ and the function $\rho(z)$ given by (6.6) drifts with velocity u without changing its shape. Any other initial distribution will be deformed for $\mu > 0$ in the course of the drift process and will go over to (6.6) only as $t \to \infty$. Thus, a sufficiently long cell is necessary if the distribution (6.6) is to be recorded (see Conclusion).

7. EFFECT OF THE RADIATION AND MEDIUM PARAMETERS ON THE EVOLUTION OF THE PARTICLE-DENSITY DISTRIBUTION

The formulas given by (4.14) and (6.6) show that the amplitude ($\sim \Delta u$) and width ($D/|\Delta u|$) of the solitary wave are determined by the drift velocity jump Δu, described by (3.8), (3.9), and (6.4). When $\partial u(z,t)/\partial N(z,t) \neq 0$, the dependence of the width and amplitude of the solitary wave on the radiation intensity is determined by G and G^{-1}, respectively. The LID effect is characterized by the following dependence of the width of the solitary wave (4.14):

$$G=(1+\varkappa_0)^3(1+\beta\varkappa_0)^2/\varkappa_0|1-\beta\varkappa_0^2| \tag{7.1}$$

which is shown in Fig. 9.

The evolution of the density depends on the sign of the detuning Ω and on its absolute magnitude $|\Omega|$. This is due to the dependence of the saturation parameter $\varkappa$ on $|\Omega|$. When the radiation is not monochromatic, the drift velocity $u(z,t)$ and, consequently, the evolution of the density distribution, depend on the shape of the spectrum of the radiation.[11] Here, it is also appropriate to note the strong dependence of the drift velocity on the radiation intensity in the case of periodically pulsed excitation (up to the point where the sign of the drift velocity changes[21]). This effect can be exploited in addition to the influence of the nonlinear evolution of the particle-density distribution.

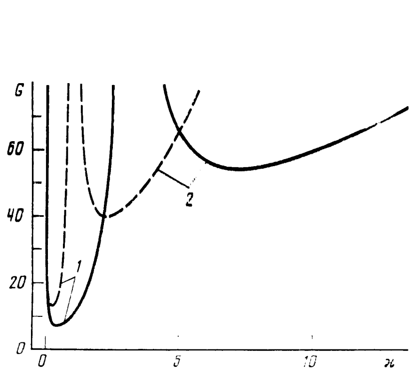

FIG. 9. Width of solitary wave as a function of radiation intensity. Curve 1—$\Omega\Delta\nu < 0$, 2—$\Omega\Delta\nu > 0$; solid curve—$\beta = 0.1$; broken curve $\beta = 1$.

The dynamics of the evolution of the density distribution will also depend on the pressure of both the absorbing and buffer gases. By varying the absorbing-gas pressure, we can vary the nonlinearity parameter σN (3.6) and thus ensure a continuous transition from an optically thin to the optically thick medium. This transition was shown in Section 2 to introduce additional (so far not fully explained) qualitative features in the drift dynamics. The dependence of the effects discussed here on the buffer-gas pressure can also be understood in the light of the fact that the buffer-gas density has a considerable influence on the magnitude of the drift velocity and on its sign.[5,13] In the case of the LID effect, the dependence of the direction of $\mathbf{u}$ on the buffer-gas pressure is possible owing to the hyperfine level splitting.[13] In the case of the radiation pressure effect, this dependence is possible owing to the negative light pressure effect[5] (see Section 2).

Finally, we note the following important point. The main parameter governing the dynamics of the evolution of the absorbing-particle distribution $\rho(z,t)$ is the drift velocity jump Δu. We have calculated the specific form of Δu in the limit of collisional broadening $\Gamma \gg k\bar{v}$. However, in principle, the parameter Δu can be found for an arbitrary ratio of the collisional (Γ) to Doppler ($\mathbf{k}\cdot\mathbf{v}$) absorption linewidths (for example, in the model of strong collisions[7] or for the Keilson-Storer collision integral[14]). Up to the stage at which Δu is calculated, our theory is valid for any ratio of Γ and $k\bar{v}$.

8. CONCLUSION

Let us now examine the possible experimental detection of the effects discussed above. We shall confine our attention to an analysis of the conditions for the appearance of the solitary wave (4.14). We shall consider the case where the width a_0 of the initial distribution $\rho(z,0)$ is less than the width $D/|\Delta u|$ of the solitary wave (4.14):

$$a_0 < \frac{D}{|\Delta u|} = \frac{D}{u_c}\frac{u_c}{\Delta u} \sim (l_{\text{LID}} l_{\text{ph}})^{1/2}. \tag{8.1}$$

In this expression, $l_{\text{ph}} \sim 1/\sigma\rho_0$ and $l_{\text{LID}} = D/u_c$ are, respectively, the photoabsorption length and the effective thickness of the layer in which the absorbing particles are compressed under the influence of the LID phenomenon. When $a_0 < D/|\Delta u|$, the initial distribution $\rho(z,0)$ is deformed into the solitary wave (4.14) in a time

$$t \gg D/(\Delta u)^2 > l_{\text{ph}}/u_c. \tag{8.2}$$

It is readily shown from (8.1) that, in the time (8.2), the gas clump will drift over the distance $\Delta z = tu_c \gg l_{\text{ph}}$. For the D-lines of alkali metals, $\sigma \sim 10^{-12}$ cm^2. When $\sigma_0 \sim 10^{12}$ cm^{-3}, this photoabsorption cross section corresponds to $l_{\text{ph}} \sim 1$ cm. The solitary wave (4.14) is thus seen to succeed in evolving in a cell of length of the order of $\Delta z \sim 10 l_{\text{ph}} \sim 10$ cm.

Experimental studies of the LID phenomenon in sodium vapor[3,15–17] have confirmed the existence of the two effects that weaken LID to a greater or lesser extent. They are physical adsorption of alkali metal vapor by the cell walls[15,16] and loss of alkali metal atoms due to chemical binding of these atoms to chemically active impurities.[3,17] The first of these was practically completely excluded by using special coatings on the cell walls.[3,17] We must now estimate the contribution of the second effect, which can be formally taken into account by adding the terms $N(z,t)/\tau_0$ (Ref. 17) or $u(z,t)/\tau_0$ to the left-hand side of (3.5) or (3.10). When the gas-filled cell is carefully freed from harmful impurities, one can readily obtain an alkali metal atomic vapor lifetime $\tau_0 \sim 1$ s. The necessary condition for observing the solitary wave is that the effective length $\Delta z \sim 10 l_{\rm ph}$ over which the solitary wave evolves not exceed the length of the region in which the alkali metal atoms are present ($\sim u_c \tau_0$), i.e., $\Delta z < u_c \tau_0$. The value $u_c \sim 1000$ cm/s was achieved in the experiment with sodium vapor,[3] from which we find that $u_c \tau_0 \sim 1000\ \text{cm} \gg \Delta z \sim 10$ cm.

It is our pleasant duty to thank S. N. Atutov, A. E. Bakarev, S.P. Pod'yachev, and A. M. Shalagin for valuable suggestions and help with this research.

APPENDIX

The matrix elements of the densities $\rho_i(v) \equiv \rho_{ii}(v)$ and $\rho_{10}(v)$ in the two-level absorbing gas obey the following set of equations[14]:

$$\begin{aligned}
&(\partial/\partial t+\Gamma_1+\mathbf{v}\cdot\nabla)\rho_1(\mathbf{v})=S_1(\mathbf{v})-2\,\mathrm{Re}\,[iG^*\rho_{10}(\mathbf{v}-\mathbf{v}_r/2)],\\
&(\partial/\partial t+\mathbf{v}\cdot\nabla)\rho(\mathbf{v})=(\hat{\Gamma}_1-\Gamma_1)\rho_1(\mathbf{v})+S_0(\mathbf{v})+S_1(\mathbf{v})\\
&\qquad+2\,\mathrm{Re}\,[iG^*\{\rho_{10}(\mathbf{v}+\mathbf{v}_r/2)-\rho_{10}(\mathbf{v}-\mathbf{v}_r/2)\}], \qquad \text{(A1)}\\
&[\partial/\partial t+\Gamma-i(\Omega-\mathbf{k}\cdot\mathbf{v})+\mathbf{v}\cdot\nabla]\rho_{10}(\mathbf{v})\\
&\qquad=iG[\rho_0(\mathbf{v}-\mathbf{v}_r/2)-\rho_1(\mathbf{v}+\mathbf{v}_r/2)],
\end{aligned}$$

where $\rho(v) = \rho_0(v) + \rho_1(v)$ and the subscripts 0 and 1 refer, respectively, to the ground and excited states of the absorbing particles. In the limit considered here ($\rho \ll \rho_b$, where ρ_b is the buffer-gas density), $S_i(v)$ is the collision integral for particles of type $i = 0, 1$ and buffer-gas particles. The integral operator

$$\hat{\Gamma}_1\rho_1(\mathbf{v})=\Gamma_1\int\rho_1(\mathbf{v}+\mathbf{v}_r/2)\cdot d\,\mathbf{k}/4\pi k$$

describes the recoil effect in the spontaneous decay of the excited state.

In this paper, we have been concerned with the macroscopic properties of the absorbing gas as a whole, namely,

$$\rho=\int\rho(\mathbf{v})\,d\mathbf{v},\quad \mathbf{j}=\int\mathbf{v}\cdot\rho(\mathbf{v})\,d\mathbf{v},$$

which remained practically constant over microscopic times Γ_1^{-1}, ν^{-1}, and Γ^{-1}. This enabled us to neglect the time derivative in the first and second equations in (A1). In the case of collisional broadening, $\Gamma \gg k\bar{v}$ and, if we use the simplifying assumptions $\Gamma_1 \ll \Gamma$, $\Delta\nu \ll \nu$, we obtain[4] the following hydrodynamic equations from (A1):

$$\begin{aligned}
&\partial\rho/\partial t+\mathrm{div}\,\mathbf{j}=0, \qquad \text{(A2)}\\
&\mathbf{j}=\mathbf{u}\rho-D\nabla\rho+\frac{D\Delta\nu}{2(\Gamma_1+\nu)(1+\beta\varkappa)}\nabla\left(\frac{\varkappa\rho}{1+\varkappa}\right).
\end{aligned}$$

In this equation, $\mathbf{u}$ is the drift velocity (2.1) and $D = \bar{v}^2/2\nu$ is the diffusion coefficient. The last term in the expression for the current density $\mathbf{j}$ describes the diffusional injection or extraction of particles into the light beam.[18] We shall not take this term into account, which is valid whenever the characteristic scale a of the spatial gradient satisfies the inequality

$$\frac{\Delta\nu}{\Gamma_1+\nu}\frac{\varkappa}{1+\varkappa}\ll\frac{ua}{D}. \qquad \text{(A3)}$$

This scale must be understood as the smaller of the two quantities a_0 and a_f, where a_0 is the initial longitudinal size of the gas clump and a_s is its final size, $\sim D/|\Delta u|$ (see (4.14)].

[1]F. Kh. Gel'mukhanov and A. M. Shalagin, Pis'ma Zh. Eksp. Teor. Fiz. **29**, 773 (1979) [JETP Lett. **29**, 711 (1979)].
[2]F. Kh. Gel'mukhanov, Avtometriya No. 1, 49 (1985).
[3]S. N. Atutov, S. Lesyak, S. P. Pod'yachev, and A. M. Shalagin, Preprint IAiE SO AN SSSR No. 321, 1986.
[4]F. Kh. Gel'mukhanov and A.M. Shalagin, Zh. Eksp. Teor. Fiz. **78**, 1674 (1980) [Sov. Phys. JETP **51**, 839 (1907)].
[5]F. Kh. Gel'mukhanov, Kvantovaya Elektron. (Moscow) **8**, 1881 (1981) [Sov. J. Quantum Electron. **11**, 1138 (1981)].
[6]V. S. Letokhov and V. G. Minogin, Phys. Rep. **73**, 1 (1981).
[7]F. Kh. Gel'mukhanov and A. M. Shalagin, Kvantovaya Elektron. (Moscow) **8**, 590 (1981) [Sov. J. Quantum Electron. **11**, 357 (1981)].
[8]G. B. Whitham, *Linear and Nonlinear Waves*, Wiley, New York, 1974 [Russian translation, Nauka, Moscow, 1973].
[10]G. Nienhuis, Phys. Rev. A **31**, 1636 (1985).
[11]A. K. Popov, A. M. Shalagin, V. M. Shalaev, and V. Z. Yakhnin, Zh. Eksp. Teor. Fiz. **80**, 2175 (1981) [Sov. Phys. JETP **53**, 1134 (1981)].
[12]A. K. Popov, V. M. Shalaev, and V. Z. Yakhnin, Zh. Eksp. Teor. Fiz. **82**, 725 (1982) [Sov. Phys. JETP **55**, 431 (1982)].
[13]A. I. Parkhomenko and A. M. Shalagin, Preprint IAiE SO AN SSSR No. 225, 1984.
[14]S. G. Rautian, G. I. Smirnov, and A. M. Shalagin, Nelineinye rezonansy v spektrakh atomov i molekul (Nonlinear Resonances in the Spectra of Atoms and Molecules), Nauka, Novosibirsk, 1979.
[15]V. D. Antsygin, S. N. Atutov, F. Kh. Gel'mukhanov *et al.*, Pis'ma Zh. Eksp. Teor. Fiz. **30**, 262 (1979) [JETP Lett. **30**, 243 (1979)].
[16]H. G. C. Werij, J. P. Woerdman, J. J. Beenakker, and I. Kušcer, Phys. Rev. Lett. **52**, 2237 (1984).
[17]S. N. Atutov, Preprint IAiE SO AN SSSR No. 288, 1985.
[18]F. Kh. Gel'mukhanov and A. M. Shalagin, Zh. Eksp. Teor. Fiz. **77**, 461 (1979) [Sov. Phys. JETP **50**, 234 (1979)].

Translated by S. Chomet